

Eggshell membrane modulates gut microbiota to prevent murine pre-cachexia through suppression of T helper cell differentiation

Huijuan Jia^{1*}, Weida Lyu¹, Kazuki Hirota¹, Eri Saito¹, Moe Miyoshi¹, Hirohiko Hohjoh², Kyohei Furukawa¹, Kenji Saito¹, Makoto Haritani³, Akashi Taguchi⁴, Yukio Hasebe⁵ & Hisanori Kato^{1*} 

¹Health Nutrition, Graduate School of Agricultural and Life Sciences, University of Tokyo, Tokyo, Japan; ²National Institute of Neuroscience, NCNP, Tokyo, Japan;

³Environmental Science for Sustainable Development Graduate School of Agriculture and Life Sciences, University of Tokyo, Tokyo, Japan; ⁴Research Center for Advanced Science and Technology, University of Tokyo, Tokyo, Japan; ⁵ALMADO Inc., Tokyo, Japan

Abstract

Background Cachexia is a life-threatening condition observed in several pathologies, such as cancer or chronic diseases. Interleukin 10 (*Il10*) gene transfer is known to improve cachexia by downregulating *Il6*. Here, we used an IL10-knockout mouse model to simulate cachexia and investigate the effects of eggshell membrane (ESM), a resistant protein, on general pre-cachexia symptoms, which is particularly important for the development of cachexia therapeutics.

Methods Five-week-old male C57BL6/J mice were fed an AIN-93G powdered diet (WT), and 5-week-old male B6.129P2-*Il10* ^{<tm1Cgn>/J} (*Il10*^{-/-}) mice were fed either the AIN-93G diet (KO) or an 8% ESM-containing diet (KOE) for 28 weeks. The tissue weight and levels of anaemia-, blood glucose-, lipid metabolism-, and muscular and colonic inflammation-related biochemical markers were measured. Transcriptomic analysis on liver and colon mucus and proteomic analysis on skeletal muscle were performed. Ingenuity Pathway Analysis was used to identify molecular pathways and networks. Caecal short-chain fatty acids (SCFAs) were identified using HPLC, and caecal bacteria DNA were subjected to metagenomic analysis. Flow cytometry analysis was performed to measure the CD4⁺ IL17⁺ T cells in mesenteric lymph nodes.

Results The body weight, weight of gastrocnemius muscle and fat tissues, colon weight/length ratio, plasma HDL and NEFA, muscular PECAM-1 levels ($P < 0.01$), plasma glucose and colonic mucosal myeloperoxidase activity ($P < 0.05$) and T helper (Th) 17 cell abundance ($P = 0.071$) were improved in KOE mice over KO mice. Proteomic analysis indicated the protective role of ESM in muscle weakness and maintenance of muscle formation (>1.5-fold). Transcriptomic analysis revealed that ESM supplementation suppressed the LPS/IL1-mediated inhibition of RXR function pathway in the liver and downregulated the colonic mucosal expression of chemokines and Th cell differentiation-related markers ($P < 0.01$) by suppressing the upstream BATF pathway. Analysis of the intestinal microenvironment revealed that ESM supplementation ameliorated the microbial alpha diversity and the abundance of microbiota associated with the degree of inflammation ($P < 0.05$) and increased the level of total organic acids, particularly of SCFAs such as butyrate (2.3-fold), which could inhibit Th1 and Th17 production.

Conclusions ESM supplementation ameliorated the chief symptoms of cachexia, including anorexia, lean fat tissue mass, skeletal muscle wasting and reduced physical function. ESM also improved colon and skeletal muscle inflammation, lipid metabolism and microbial dysbiosis. These results along with the suppressed differentiation of Th cells could be associated with the beneficial intestinal microenvironment and, subsequently, attenuation of pre-cachexia. Our findings provide insights into the potential of ESM in complementary interventions for pre-cachexia prevention.

Keywords Cachexia; Egg shell membrane; Gut microbiota; IL10-knockout mice; SCFA; T helper cells differentiation

Received: 26 November 2021; Revised: 11 April 2022; Accepted: 9 May 2022

*Correspondence to: Hisanori Kato and Huijuan Jia, Health Nutrition, Graduate School of Agricultural and Life Sciences, University of Tokyo, Tokyo, Japan.

Email: akataq@mail.ecc.u-tokyo.ac.jp; akakeiken@g.ecc.u-tokyo.ac.jp

Introduction

Cachexia is a life-threatening condition observed in several pathologies, including cancer and chronic diseases, and it is generally divided into the 'pre-cachexia', 'cachexia' and 'refractory cachexia' stages.¹ Cachexia is mostly accompanied by anorexia, significant lean fat tissue mass, skeletal muscle wasting, reduced physical function and even increased cancer-related mortality, especially in the majority of patients with advanced-stage cancer.^{2,3} In addition, chronic inflammation is one of the major drivers of cachexia by virtue of its role in several tissue types, including fat, skeletal muscle, brain and liver tissues, mediated by pro-inflammatory cytokines such as tumour necrosis factor alpha (TNF- α), interleukin (IL) 6 and interferon gamma (IFN γ).⁴ However, the therapeutic options for cachexia are limited as cachectic patients are less tolerant to chemotherapy and radiotherapy. In contrast, researchers have expressed significant interest in pre-cachexia, the early stage of cachexia, as appropriate alleviation at this stage is considered to prevent and delay the pathogenesis of cachexia.⁵

IL10 can inhibit the expression of T cell-derived cytokines, such as IFN γ , and reduce the antigen-presenting potential of monocytes.^{6,7} Additionally, IL10 can significantly downregulate pro-inflammatory cytokines, such as IL1, IL6 and TNF- α , by preventing endotoxin-induced acute lethality.⁸ In a mice model, *Il10* gene transfer was shown to improve cachexia by downregulating *Il6* expression at the tumour sites.⁹ A previous study has reported that in humans, the IL10 genotype of the host can influence the development of cachexia, as observed among patients with gastroesophageal malignancy.¹⁰ Moreover, the gene haplotype of IL10 contributes to the occurrence of cachexia in patients with gastric cancer.¹¹

Eggshell membrane (ESM), a nontoxic and low-cost biological material, contains high levels of collagenized fibrous proteins and acts as a resistant protein with approximately 46% digestibility.¹² Ruff et al. reported the safety of ESM as a food supplement in 2012 and its roles as a consumable anti-inflammatory food product, such as maintenance of joints and connective tissues.¹³ In our previous studies, we demonstrated that ESM supplementation ameliorates intestinal inflammation by facilitating the restitution of epithelial injury and alleviating microbial dysbiosis,¹⁴ and improves hepatic fibrogenesis both in human cell lines and rodent models.¹⁵

In this study, we used IL10-knockout mice as a spontaneous inflammatory bowel disease (IBD) and colorectal cancer model to simulate the symptoms of cachexia. We investigated the effects of ESM on cachexia targeting several tissues, including liver, skeletal muscles, fat and colon. Additionally, we evaluated the changes in the gut microbiota. We demonstrated that ESM alleviated cachexia in IL10-knockout mice and the underlying mechanism could be associated with

the production of ESM metabolites by the action of gut microbiota and their regulation of T helper (Th) cell differentiation.

Methods

Animal experiments

Five-week-old male B6.129P2-IL10 $< tm1Cgn > / J$ (IL10 $^{-/-}$) mice (The Jackson Laboratory, Bar Harbor, ME) were fed an American Institute of Nutrition in 1993 (AIN-93G) powdered diet (KO) or an 8% ESM-containing AIN-93G diet (KOE) ($n = 7$) for 28 weeks (Table S1). C57BL/6 wild-type mice (Oriental Yeast Co., Ltd., Tokyo, Japan) were fed the AIN-93G diet and used as normal controls (WT) ($n = 5$). The experiment was conducted at a controlled temperature ($23 \pm 2^\circ\text{C}$), relative humidity (50–60%) and lighting condition (12-h light/dark cycle). The general characteristic indices, including body weight, food intake and stool consistency, were measured. The stool consistency score was determined as follows: 0, normal; 2, soft; 4, diarrhoea. The study protocol was approved by the Animal Care and Use Committee of the University of Tokyo, and the animals were treated with humane care, in accordance with the committee's guidelines.

Blood collection and tissue harvesting

Mice were anaesthetized with pentobarbital sodium upon the termination of the experiment prior to euthanization and then bled from the carotid artery. The plasma and red blood cells were isolated by centrifugation at $1000 \times g$ for 15 min at 4°C . The distance between the ileocecal junction and the proximal rectum was measured and considered the colon length. The liver, colon, spleen, mesenteric fat, retroperitoneal fat, epididymal fat, gastrocnemius muscle and caecum contents were frozen in liquid nitrogen and stored at -80°C until further analysis.

Biochemical assays

The haemoglobin levels in blood cells were measured using a haemoglobin assay kit (Wako Pure Chemical Industries, Osaka, Japan). Total lipids were extracted from the liver using the Folch method. Plasma and hepatic total cholesterol (TC), triglyceride (TG), high-density lipoprotein (HDL) cholesterol and non-esterified fatty acid (NEFA) levels and plasma glucose levels were measured using Wako kits. Plasma insulin levels were measured using a kit from the Morinaga Institute of Biological Science (Yokohama, Japan). Mucosal myeloperoxidase (MPO) activity was measured using a colorimetric

kit (BioVision, Palo Alto, CA, USA) according to the manufacturer's instructions.

Histology

Colon histopathology

Colonic tissue slices from the mice in each group were embedded in optimal cutting temperature compound (Sakura Finetek, Torrance, CA, USA) and snap-frozen in liquid nitrogen. Each 5- μ m-thick slice of tissue was sectioned and stained with haematoxylin and eosin and subjected to light microscopy (Olympus BX51 microscope, Olympus Optical, Tokyo, Japan).

Muscle immunohistochemistry

Muscle tissue sections were treated with an anti-PECAM-1 rabbit polyclonal antibody (Spring Bioscience) and scored based on observations from five different fields per sample. The number of positively stained cells was expressed as the average of the total percentage area of cells at 20 \times magnification using ImageJ (<http://rsbweb.nih.gov/ij/>) by two independent investigators blinded to the experimental conditions.

NanoLC-MS/MS proteomic analysis and western blotting analysis

Proteomic analysis of the gastrocnemius muscle using an isobaric tag for relative and absolute quantitation (iTRAQ) and western blotting analysis of liver proteins were conducted according to procedures described in the Supporting Information.

Transcriptomic analysis

DNA microarray analysis and Ingenuity Pathway Analysis

Microarray analyses (Affymetrix Mouse Genome 430 2.0 Array GeneChips, Santa Clara, CA, USA) were performed using pooled total liver or colon mucosal RNA extracted using an RNA Isolation Kit (NucleoSpin[®] RNA II, Macherey-Nagel, Düren, Germany) and TRIzol reagent (Invitrogen, Carlsbad, CA, USA), respectively, from mice from each group. The scanned images were analysed using Affymetrix Microarray Suite Ver. 5.0 to calculate the gene expression ratios for KO versus CON mice and KOE versus KO mice. The differentially expressed genes were defined as those with expression log (ratio) > 1.0 and < -1.0 and mapped using the Ingenuity Pathway Analysis's (IPA) Pathway Explorer function.

Validation of gene expression

Real-time reverse transcription polymerase chain reaction (RT-PCR) and digital polymerase chain reaction (dPCR) were

performed to confirm the expression of differentially expressed genes; the sequences of the primers used are shown in Table S2.

Caecal metagenomic analysis and measurement of caecal short-chain fatty acid concentrations

16S rDNA sequencing and caecal short-chain fatty acid (SCFA) measurement were performed according to methods described in our previous study¹⁶ (Supporting Information).

Flow cytometry analysis of mesenteric lymph nodes

Flow cytometry analysis was performed according to a routine procedure (Supporting Information) using FACSverse (BD Biosciences, San Jose, CA, USA).

Statistical analyses

Data are presented as mean \pm standard error (SE) and analysed using one-way analysis of variance. Significant differences were evaluated using Tukey's test at the following levels of significance: * P < 0.05 and ** P < 0.01.

Results

General characteristics

There were no significant changes in body weight between WT and KOE mice at 28 weeks (*Figure 1A*). However, from the 21 to the 28 weeks, KO mice exhibited significant reduction in body weight compared with WT mice, and after the 23rd week, significant body weight loss was observed in KO mice compared with that in KOE mice, with a final survival rate of 70 and 82%, respectively.

No significant differences were observed in the average daily food intake among the WT, KO and KOE mice during the whole experimental period (*Figure 1B*). However, the average daily food intake in the KO group was significantly lower than that in the WT group from the 14th week to the 28th week and was lower during the 14th and 18th weeks compared with that in the KOE group.

With respect to stool consistency, KO mice exhibited soft stool formation from the 13th week, which tended to increase till the 28th week (*Figure 1C*). KOE mice exhibited soft stool formation from the 23rd week, and the degree of softness was significantly lower than that in KO mice.

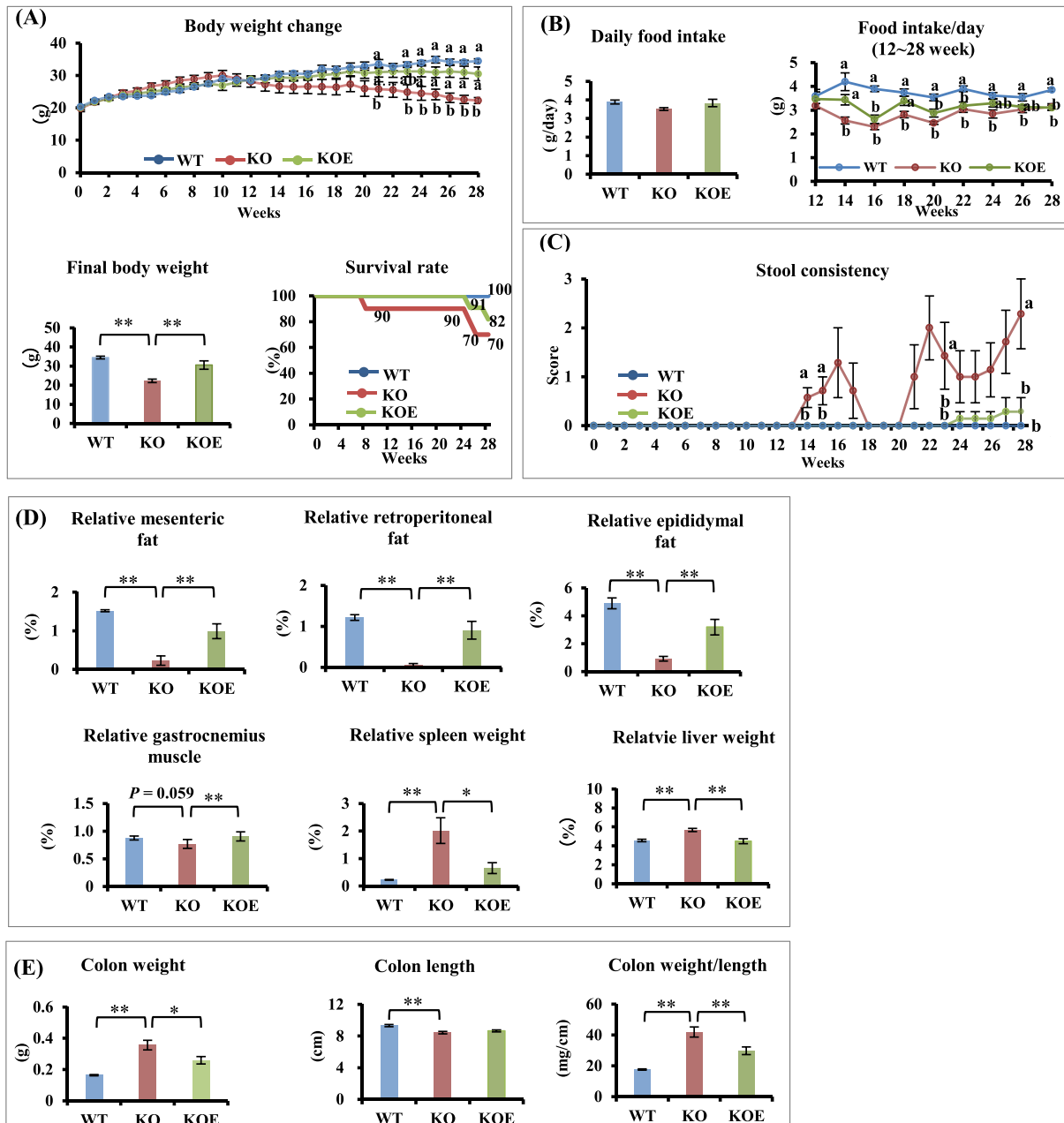


Figure 1 General characteristics. (A) Body weight changes, final body weight and survival rate. (B) Daily food intake and food intake since 12th week. (C) Stool consistency changes. (D) Relative weights of mesenteric fat, retroperitoneal fat, epididymal fat, gastrocnemius muscle, spleen and liver. (E) Colon weight, colon length and the ratio of colon weight to length. KO, IL10 KO mice; KOE, IL10 KO mice supplemented with ESM; WT, wild-type mice. All values are mean \pm SE ($n = 5-7$). Data with different letters (a,b,c) are significantly different at $P < 0.05$, or $*P < 0.05$ and $**P < 0.01$ by one-way ANOVA Tukey's test.

The weights of fat tissues (Figure 1D), gastrocnemius muscle, spleen, liver and colon as well as the colon weight/length ratio (Figure 1E) were significantly altered in KO mice compared with that in WT mice; however, these factors improved considerably in response to ESM supplementation in KO mice.

Biochemical assays

The plasma glucose, HDL cholesterol and NEFA levels were significantly lower in KO mice than in WT mice, whereas the levels recovered considerably in KOE mice (Figure 2A). No significant changes were observed in the plasma insulin, TG and

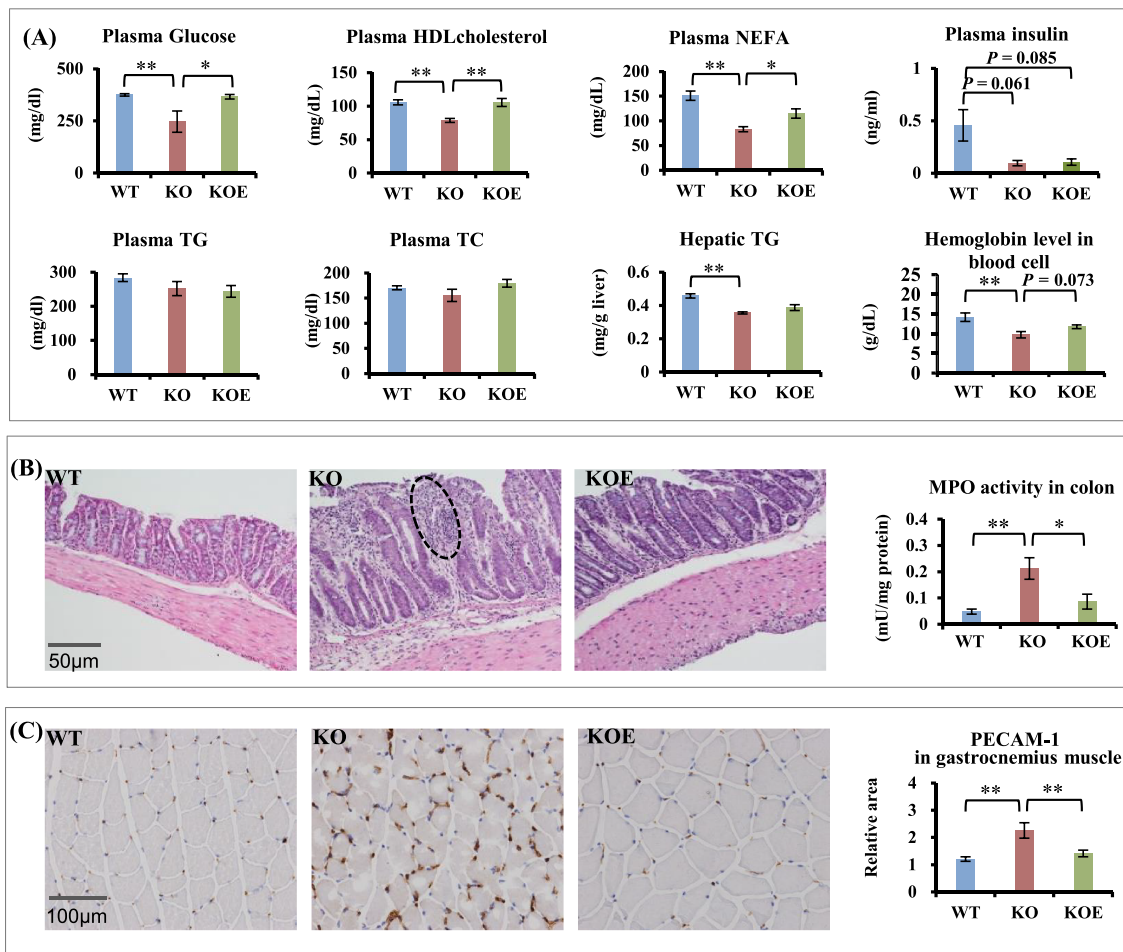


Figure 2 Biochemical and histochemical analyses. (A) Plasma glucose, HDL cholesterol, NEFA, insulin, TG, TC, hepatic TG and haemoglobin levels in red blood cells. (B) Haematoxylin and eosin (H&E) staining of colon and MPO activity. (C) Immunohistochemistry of PECAM1 in gastrocnemius muscle. KO, IL10 KO mice; KOE, IL10 KO mice supplemented with ESM; WT, wild-type mice. All values are mean \pm SE ($n = 5-7$). * $P < 0.05$ and ** $P < 0.01$ by one-way ANOVA Tukey's test.

TC levels or the hepatic lipid metabolism markers between the KO and KOE groups. The haemoglobin level in red blood cells was significantly lower in KO mice than in WT mice, whereas it tended to increase in KOE mice ($P = 0.073$).

Colon and muscle parameters

IL10 knockout induced a structural disorder in mucosal epithelial cells, which may have increased the infiltration of inflammatory cells into the mucosa and submucosa. ESM supplementation clearly ameliorated this disorder by reducing inflammatory cell infiltration (Figure 2B), which was also reflected in the lower mucosal activity of MPO, a marker of neutrophil migration, in KOE mice. In addition, the platelet endothelial cell adhesion molecule-1 (PECAM-1) levels in the muscles were significantly elevated in KO mice than in

WT mice and were significantly reduced in KOE mice, as revealed by immunohistochemical analysis (Figure 2C).

Comparative proteomic analysis of muscles using iTRAQ

We denoted the muscular proteins with >1.5 -fold change in expression as differentially expressed proteins (Table 1). Fifteen proteins were upregulated in KO mice compared with that in WT mice but downregulated in KOE mice compared with that in KO mice; these included calsequestrin-1 (CASQ1), myosin light chain 1/3 (MLC1), myozenin-1 (MYOZ1), four and a half LIM domains 1 (FHL1), tropomyosin alpha 3 chain (TPM3), troponin T (TNNT3) and galectin-1 (LGALS1). In addition, 12 proteins exhibited the opposite expression pattern,

Table 1 List of differentially expressed muscle proteins among the groups

Accession no.	Protein name, symbol	Protein symbol	KO/CON	KOE/KO
D9J303	ENH isoform 3a	PDLIM5	1.60	0.07
O09165	Calsequestrin-1	CASQ1	16.44	0.07
P51667	Myosin regulatory light chain 2	MYL2	1.20	0.16
Q9JK37	Myozenin-1	MYOZ1	4.02	0.17
E9QNP0	KxDL motif-containing protein 1	KXD1	5.35	0.19
P43277	Histone H1.3	HIST1H1D	3.31	0.29
P05977	Myosin light chain 1/3	MLC1	32.51	0.31
A2AEX8	Four and a half LIM domains 1	FHL1	1.53	0.33
E9Q5J9	Tropomyosin alpha-3 chain	TPM3	5.86	0.37
A2A6I5	Troponin T	TNNT3	1.22	0.48
Q4VWZ5	Acyl-CoA-binding protein	DBI	7.80	0.50
P16045	Galectin-1	LGALS1	1.67	0.53
Q70400	PDZ and LIM domain protein 1	PDLIM1	1.38	0.53
Q61330	Contactin-2	CNTN2	1.72	0.65
P97450	ATP synthase-coupling factor 6	ATP5PF	2.40	0.67
P68134	Actin, alpha skeletal muscle	ACTA1	0.63	1.67
P13541	Myosin-3	MYH3	0.40	1.79
P12787	Cytochrome c oxidase subunit 5A	COX5A	0.28	1.96
P11404	Fatty acid-binding protein	FABP3	0.14	2.00
Q6P1B9	Bin1 protein	BIN1	0.57	2.00
Q3UKW2	Calmodulin-1	CALM1	0.44	2.40
A6Z144	Fructose-bisphosphate aldolase	ALDOA	0.33	3.60
D3Z7A7	Formin-like protein 3	FMNL3	0.18	3.60
Q9CPU0	Lactoylglutathione lyase	GLO1	0.27	3.73
P32848	Parvalbumin alpha	PVALB	0.65	3.77
Z4YNB2	Troponin T	TNNT3	0.09	5.55
Q9D1X0	Nucleolar protein 3	NOL3	0.09	7.18

including actin alpha (ACTA1), cytochrome c oxidase subunit 5A (COX5A) and fatty acid-binding protein (FABP3).

Liver transcriptomic analysis

The differentially expressed genes (Figure S1) identified by hepatic microarray analysis were analysed using IPA; the Top 10 Ingenuity canonical pathways of KO/WT and KOE/KO mice are shown in Table S3. The lipopolysaccharide (LPS)/IL1-mediated inhibition of RXR function pathway was significantly altered in KO/WT as well as KOE/KO mice, and the expression of genes in this pathway was confirmed using RT-PCR. ESM supplementation downregulated the expressions of lipopolysaccharide-binding protein (*Lbp*), CD14 antigen (*Cd14*), Toll-like receptor 4 (*Tlr4*), interleukin 1 receptor type II (*Il1r2*), interleukin 1 beta (*Il1b*), interleukin 1 receptor-associated kinase 4 (*Irak4*), mitogen-activated protein kinase kinase kinase 1 (*Map3k1*, $P = 0.083$) and tumour necrosis factor alpha (*Tnfa*) genes (Figure 3A). Although no changes were observed in the expression of other genes, the Myd88 protein levels were lower in KOE mice ($P = 0.056$) than in KO mice (Figure 3B). Additionally, dPCR analysis revealed that the expression of *Il6*, which encodes the inflammation-related protein IL6, was significantly upregulated in KO mice than in WT mice and downregulated in KOE

mice (Figure 3C). These changes in LPS/IL1-mediated inhibition of RXR function pathway is summarized in Figure 3D.

Microbiota dysbiosis and community structure

Hierarchical clustering dendrogram analysis was performed to investigate the gut microbiota composition in each group. The gut microbiota composition of KOE mice was more similar to that of WT mice than KO mice (Figure 4A). This result is similar to that of principal coordinates analysis (PCoA) (Figure 4B) in which the differences in the distribution of taxa among samples were identified up to a fixed taxonomic level. The Shannon diversity index analysis showed that ESM supplementation increased the alpha diversity of the microbiota in IL10-knockout mice compared with that in KO mice; additionally, obvious differences were noted in the Chao1 indices (Figure 4C).

ESM supplementation significantly increased the relative abundances of Bacteroidetes (one of the most abundant phyla), Firmicutes (colitis-related bacteria), Verrucomicrobia and *Deferribacteraceae* (DSS-induced colitis-related bacteria) (Figure 4D). The relative abundances of *Akkermansia muciniphila* (inducer of intestinal inflammation) and the pathogenicity of *Bacteroidaceae* and *Porphyromonadaceae* (opportunistic pathogens), *Bacteroides ovatus* (inducer of gut tissue inflammation) and *Bacteroides acidifaciens* (promoter of

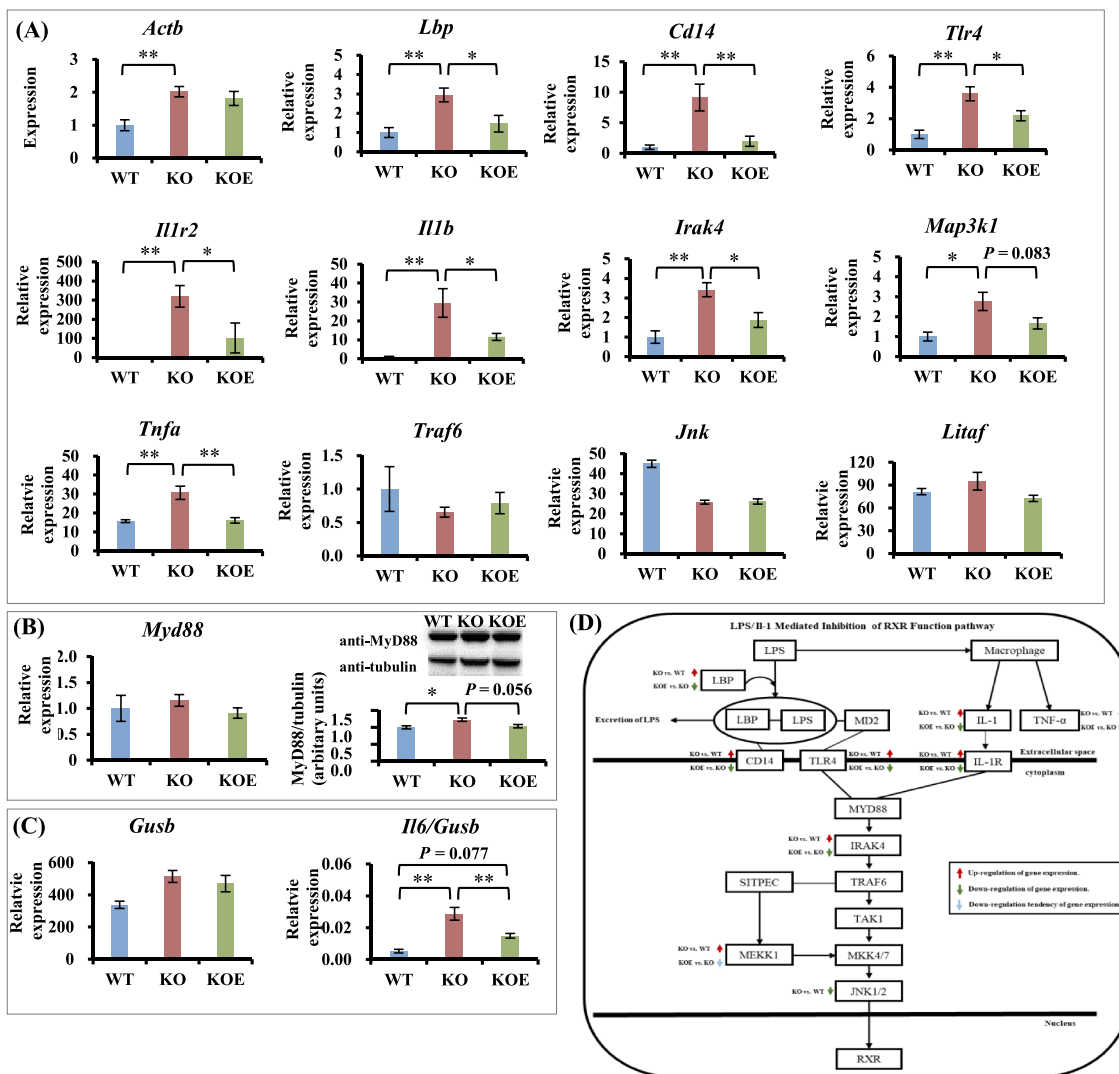


Figure 3 Hepatic changes. (A) mRNA expression of genes measured by RT-PCR and normalized to Actb. (B) mRNA expression and protein level of Myd88 by western blotting normalized to tubulin. (C) Il6 expression measured by dPCR and normalized to Gusb. (D) Schematic representation of LPS/IL1-mediated inhibition of RXR function pathway. KO, IL10 KO mice; KOE, IL10 KO mice supplemented with ESM; WT, wild-type mice. All values are mean \pm SE ($n = 5-7$). * $P < 0.05$ and ** $P < 0.01$ by one-way ANOVA Tukey's test.

IgA production) were increased in response to IL10 knockout and decreased in response to ESM supplementation. The relative abundance of *Ruminococcaceae*, which are enteric SCFA fermenters, increased significantly in KOE mice compared with that in KO mice (Table S4D).

Changes in caecal SCFA concentration

IL10 knockout significantly decreased the caecal acetate and butyrate levels and increased the lactate and isobutyrate levels compared with those in WT mice (Figure 4E), whereas ESM supplementation significantly increased the butyrate and acetate levels, as well as total SCFA level compared with those in KO mice. The valeric acid concentration was unal-

tered by IL10 knockout but was significantly increased by ESM supplementation compared with that in WT mice. No significant changes were observed in the caecal propionic acid and isovaleric acid concentrations among the groups.

Colon mucus transcriptomic analysis

The differentially expressed genes (Figure S2) identified in the colonic microarray analysis were analysed using IPA for identifying the related biological functions and pathways. The Top 10 Ingenuity canonical pathways of KO/WT and KOE/KO mice are shown in Table S4. Compared with that in KO mice, ESM supplementation downregulated inflammation-related genes in the colon mucosa, including

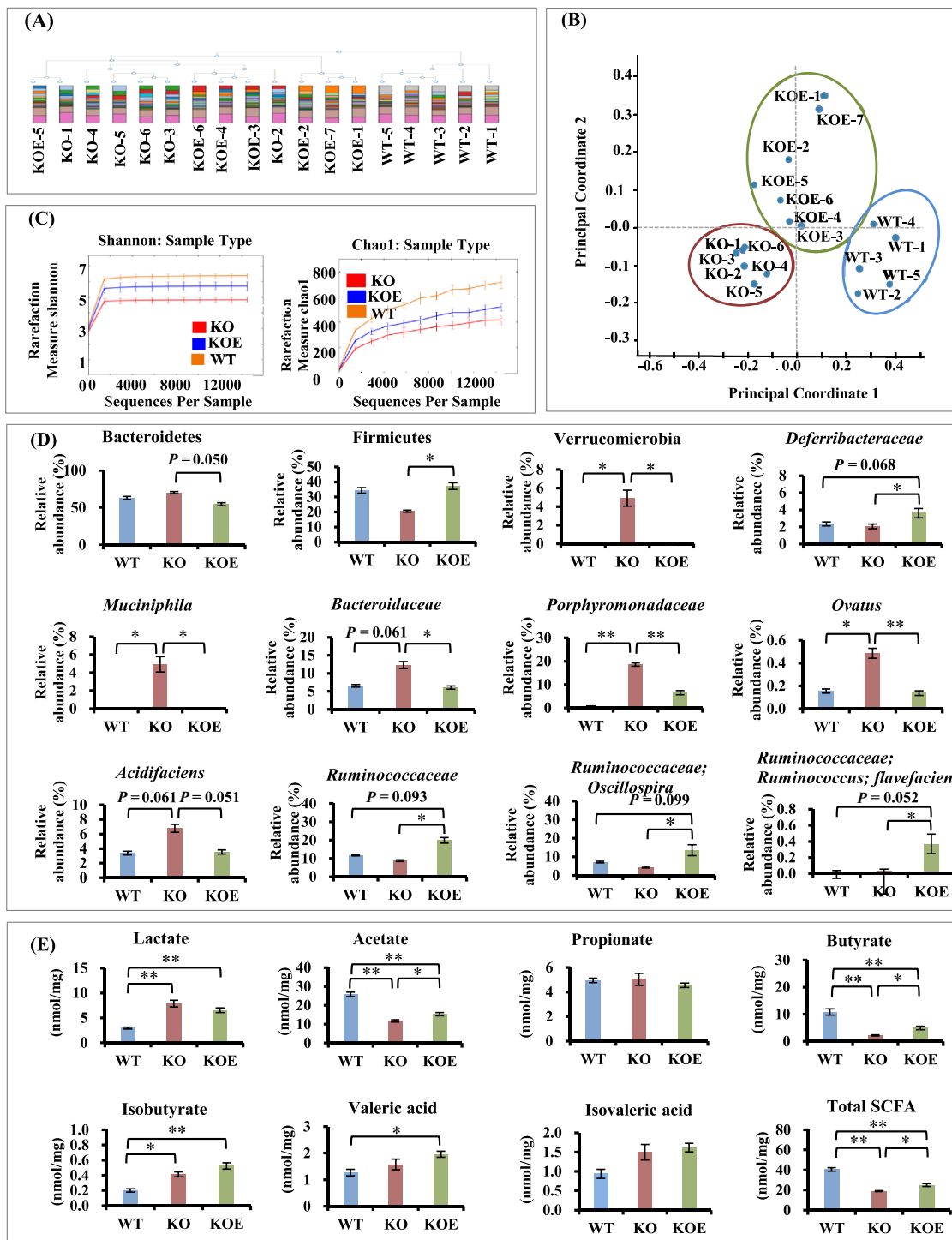


Figure 4 Changes of intestinal environment in caecal samples. (A) Hierarchical clustering dendrogram analysis. (B) Principal coordinates analysis (PCoA) measurement at the genus level. (C) Alpha diversity analysis using the Shannon diversity index and alpha diversity analysis using the Chao1 diversity index. (D) The relative abundance of bacteria. (E) Concentration of organic acids. KO, IL10 KO mice; KOE, IL10 KO mice supplemented with ESM; WT, wild-type mice. All values are mean ± SE (n = 5–7). *P < 0.05 and **P < 0.01 by one-way ANOVA Tukey's test.

chemokine (C-C motif) ligand 9 (*Ccl9*), chemokine (C-C motif) receptor 1 (*Ccr1*), members of chemokine (C-X-C motif) ligand family (*Cxcl13* and *Cxcl11*), chemokine (C-X-C motif) receptor

5 (*Cxcr5*), *Il6*, interleukin 12 (*Il12a*, *Il12b*) and interleukin 12 receptor (*Il12rb1*) (Figure 5A). In addition, the expression of T-cell differentiation-related genes was suppressed in KOE

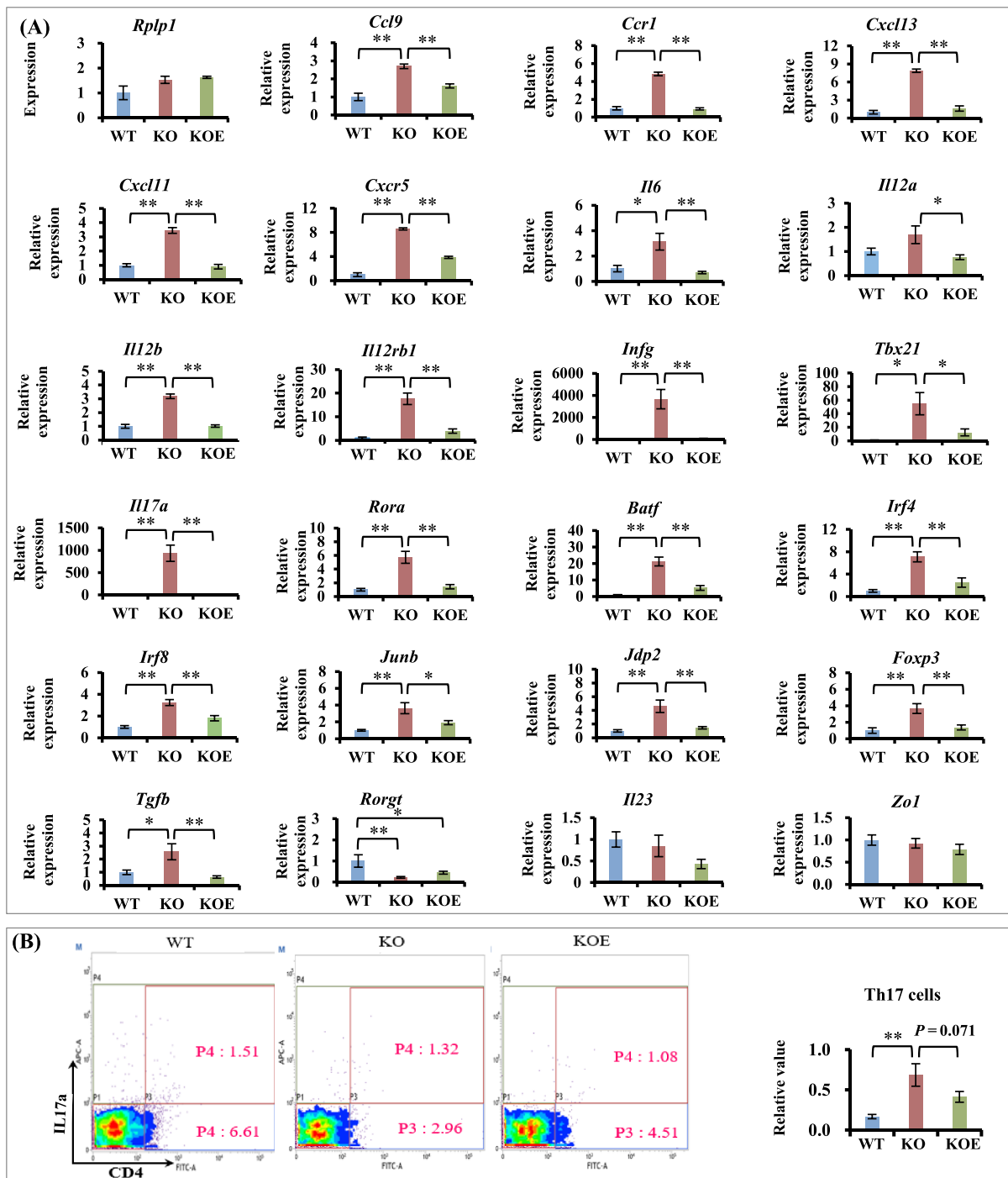


Figure 5 Changes in colonic mucosa and mesenteric lymph nodes. (A) mRNA expression of colonic mucosal genes measured by RT-PCR and normalized to *Rpl1*. (B) Quantification of Th17 cells in mesenteric lymph nodes by flow cytometry. KO, IL10 KO mice; KOE, IL10 KO mice supplemented with ESM; WT, wild-type mice. All values are mean \pm SE ($n = 5-7$). * $P < 0.05$ and ** $P < 0.01$ by one-way ANOVA Tukey's test.

mice. These genes are related to Th1 cell development including *Infg* and T-box protein 21 (*Tbx21*); Th17 cell development including interleukin 17 (*Il17a*), retinoid-related orphan receptor (*Rora*), basic leucine zipper transcription factor ATF-like (*Batf*), interferon regulatory factor (*Irf4*, *Irf8*), tran-

scription factor jun-B (*Junb*) and JUN dimerization protein 2 (*Jdp2*); regulatory T cell (*Treg*) development including its transcription factor forkhead box P3 (*FoxP3*); and *Treg*/Th17 balance maintenance including transforming growth factor (*Tgfb*) and *Il6*. However, no significant changes between the

KO and KOE groups were observed in the expression of retinoic acid receptor-related orphan receptor gamma t (*Rorgt*), *Il23* and zonula occludens 1 (*Zo1*) (Figure 5A), which are associated with intestinal barrier function.

Changes in the abundance of Th17 cells

KO mice showed a significantly high CD4⁺IL17A frequency in mesenteric lymph nodes (MLNs), which tended to be attenuated ($P = 0.071$) by ESM supplementation in KOE mice (Figure 5B).

Discussion

Cachexia is primarily accompanied by symptoms such as anorexia, significant lean fat tissue mass, skeletal muscle wasting, reduced physical function and increased cancer-related mortality.^{2,3,17} Our results demonstrated that the IL10-knockout mice mimicked the symptoms of cachexia, including anorexia (from 14 to 28 weeks), obvious loss in both fat tissue and skeletal muscle and dysfunction in skeletal muscles, gut and liver, as indicated by proteomic, transcriptomic and microbiota analyses. ESM supplementation significantly ameliorated these symptoms as well as the symptoms of IBD, including body weight loss, stool consistency, colon weight/length ratio and MPO activity. According to previous reports, anorexia is mostly characterized by TNF- α expression,¹⁸ and muscle weight loss may result from the synergistic relationship among TNF- α , IFN γ , and IL1.^{19,20} In this study, ESM supplementation significantly downregulated the expressions of *Tnfa* and *Il1b* in the liver, which is consistent with the results of food intake in the specific period and muscle weight.

Proteomic analysis revealed that ESM supplementation considerably improved muscle weakness and maintenance of muscle formation. The differentially expressed genes among the groups encode proteins with the following functions. TPM3, in association with the troponin complex, plays a critical role in the calcium-dependent regulation of vertebrate striated muscle contraction. Reportedly, dominant mutations in *Tpm3* may cause congenital myopathy, characterized by generalized muscle weakness, by inducing α -tropomyosin expression.²¹ Abnormal cross-bridge cycling kinetics and Ca²⁺ sensitivity was observed in the contraction of single skeletal myofibres isolated from biopsies of patients with dominant *Tpm3* mutations.²² TNNT3 overexpression may lead to the loss of thin filaments and markedly altered muscle formation.²³ ACTA1 forms the core of the thin filament of sarcomeres and generates contractile force in muscles.²⁴

IL10 knockdown upregulated CASQ1, MLC1, MYOZ1, and FHL1, which regulate the entry of calcium stored in skeletal

muscle and maintain muscle function via anti-inflammatory action. CASQ1 is a Ca²⁺-binding proteins that restores the function and structure of calcium release units in skeletal muscles.²⁵ MLC1 maintains myofibres and muscle function.²⁶ MYOZ1, expressed in fast-twitch fibres of skeletal muscles, maintains calcineurin function and substrate specificity and contributes to calcium-dependent signal transduction.²⁷ *Fhl1* deletions are associated with rare hereditary myopathies and cardiomyopathies.²⁸ The significant downregulation of these proteins in KOE mice may indirectly indicate ESM-induced muscle maintenance.

Additionally, *Lgals1* overexpression was found to be harmful, as observed in KO mice, in contrast to that in WT mice. LGALS1, commonly overexpressed in malignant cancers, mediates cancer progression by interacting with glycoconjugates in the tumour microenvironment. *Lgals1* upregulation in KO mice was ameliorated by ESM supplementation, indicating muscle maintenance by ESM. *Cox5a* downregulation leads to mitochondrial dysfunction by reducing the mitochondrial complex IV activity and cellular ATP content.²⁹ Partially *Fabp3*-deficient mice exhibited reduced fatty acid utilization.³⁰ *Cox5a* and *Fabp3* downregulation in KO mice may have hindered muscle contraction through poor energy utilization, and ESM supplementation significantly upregulated these proteins.

PECAM-1 is localized to the intercellular junctions of endothelial cells and the surface of human platelets. Higher concentrations of PECAM-1 are associated with the transmigration of leukocytes into inflamed tissues, such as those abundant in patients with IBD, and the degree of expression is correlated with disease activity.³¹ The significantly low PECAM-1 level in KOE mice indicated leukocyte transmigration to the site of inflammation in muscles, which could be one of the potential reasons for muscle weight recovery by ESM supplementation. Additionally, these data suggest that high PECAM-1 levels may serve as a useful predictive marker for the induction and maintenance of inflammation in patients with cachexia.

Liver mass has been shown to increase both during cachexia progression and in colorectal cancer.³² Under these conditions, the hepatic energy expenditure increases and results in cachexia and also leads to inflammation mediated by IL6 and TNF- α , which may be one of the primary reasons for muscle loss.³³ Additionally, LPS, which is one of the primary components of the bacterial outer membrane, is combined with Lbp in plasma, delivered to the cell surface receptor CD14, and transferred to the transmembrane signalling receptor TLR4, thereby promoting the transcription of inflammatory factors. In this study, the recovery of the relative weight of the liver and the weakened expression of LPS/IL1-mediated inhibition of RXR function pathway (downregulation of *Lbp*, *Cd14*, *Tlr4*, *Il1r2*, *Il1b*, *Tnfa*, *Irak4*, *Map3k1*, and *Il6* and lowered the levels of Myd88 protein; Figure 3D), which is considered the most common inflammatory path-

way across organs and species and contributes to the amplification of inflammatory responses,³⁴ decreased the secretion of pro-inflammatory cytokines to suppress disease activity. From a transcriptomic perspective, we found that ESM supplementation improved liver dysfunction.

Emerging evidence illustrates that gut function is related to cachexia. The gut barrier function is considered to be compromised in patients with cachexia, and inflammation increases with cachexia progression in colon cancer.^{2,35} Histopathological analysis of colonic tissue sections indicated that ESM supplementation ameliorated the degree of inflammation and repaired the structural disorder of mucosal epithelial cells, which was also reflected by the lowered MPO activity in the colon mucosa. *Ccl9*, *Ccr1*, *Cxcl11*, *Cxcl13*, and *Cxcr5* were downregulated in KOE mice. CCL9 is closely associated with the recruitment of inflammatory cells, and tumour cell metastasis and CCL9 secretion by cancerous colon cells led to the recruitment of CCR1-expressing immature myeloid cells to the liver.³⁶ Moreover, *Cxcl11*, *Cxcl13* and *Cxcr5* were reported to be significantly upregulated in rodent colitis and patients with IBD. Our findings indicated that ESM supplementation significantly improved the degree of inflammation in the colon that could delay the progression of colorectal carcinoma.

The gut microbiota play a pivotal role and may constitute a potential therapeutic target in the initiation and development of cachexia.³⁷ The microbial richness and diversity in KO and WT mice were different, confirming the presence of gut dysbiosis in KO mice. ESM supplementation significantly restored the abundances of the phyla Bacteroidetes, Firmicutes, and Verrucomicrobia, families *Bacteroidaceae*, *Deferribacteraceae*, and *Porphyromonadaceae*, and species *B. ovatus*, *B. acidifaciens*, and *A. muciniphila*, which were detected in patients with IBD or rodent models. *Ruminococcaceae* is another notable taxon in this respect. The abundances of *Oscillospira* and *Ruminococcus flavefaciens* increased significantly in KOE mice than in KO mice, which accounted for the majority and minority of this bacterial family, respectively. *Ruminococcaceae* release ammonia or amines and improve the enteric fermentation of SCFAs, especially butyrate, which is an energy source for colonocytes and exhibits extensive anti-inflammatory activity by regulating immune cell migration, cytokine expression and cell proliferation, activation and apoptosis.³⁸ Several studies have confirmed that butyrate-producing microbial pharmabiotics are effective in IBD models and are used in clinical trials. Our present data demonstrated that ESM supplementation in KO mice significantly increased the relative abundance of *Ruminococcaceae*, the caecal concentration of butyric acid and the total SCFA content compared with that in KO mice. This is consistent with our previous finding that the abundance of *Ruminococcaceae* and the levels of SCFAs increased in DSS-induced colitis models following ESM supplementation¹⁴; in particular, this improved the marked

immunosuppression, led to significant shifts in the microbiota and attenuated colitis. Collectively, these results confirmed that a general beneficial shift in the gut microbiota improved the symptoms of cachexia in KOE mice, including an increase in weight gain and physical function and decrease in inflammation.

We next investigated how ESM and its metabolites affect the inflammatory response and immune system in mice. Emerging evidence has indicated that the administration of SCFAs at concentrations higher than the physiological levels induces effector (Th1 and Th17) and Tregs.³⁸ The effectors regulate pathogenesis by modulating immune responses and maintaining intestinal immune homeostasis. Several studies have shown that IL17 plays an important role in nearly all major autoimmune syndromes, including IBD, and its levels are increased in both the colonic mucosa and serum of patients with IBD, based on which the effectiveness of IL17-blockade therapy is being tested in patients with IBD.³⁸ We found that not only the levels of IL17-related markers, including *ROR α* , IL6 and IL17, and the number of Th17 cells, but also the levels of IFN- γ and Tbet (*Tbx21*) mRNA, which have been directly linked to Th1 cell development, were significantly reduced in response to ESM treatment. These findings suggested that the metabolites produced by ESM inhibited the IBD-inducing ability of T cells, thereby contributing to the maintenance of intestinal homeostasis.

Tregs are a type of T cells that are generated in response to butyrate synthesis and differentiate from Th cells. These cells are characterized by the expression of the intracellular transcription factor FOXP3.³⁹ Tregs regulate the homeostasis of the intestinal immune system by promoting anti-inflammatory cytokine production and negatively regulate other Th cell subsets, such as Th17 cells.³⁸ However, in contrast with previous results, our findings indicated that ESM treatment decreased the abundance of Tregs as well as the levels of Th17, as indicated by the reduced expression of *Foxp3* and *Il17a*, respectively. This is because the anti-inflammatory cytokine TGF- β , along with IL6 (a signalling protein that maintains the Treg/Th17 balance), could suppress Treg maturation and promote a predominantly Th17-mediated pro-inflammatory response.⁴⁰ With sufficient IL6 level, TGF- β can stimulate naïve T cells to differentiate into Th17 cells; in the absence of sufficient IL6 level, TGF- β stimulates naïve T-cell differentiation into Tregs.³⁸ The expression of *Il6* and *Tgfb* genes in KO mice was significantly higher than that in KOE mice, which was consistent with the results of Th17 analysis in mouse mucosa. In contrast, in KOE mice, both low levels of IL6 and TGF- β mRNA and high levels of butyrate led to significantly lower levels of IL17 and FOXP3 mRNA compared with that in KO mice.

We further investigated the regulatory factors that affect the differentiation of naïve T cells into Th17 cells. Notably, BATF, a member of the activator protein 1 (AP-1) family of transcription factors, and IRF4 were recently proposed as pi-

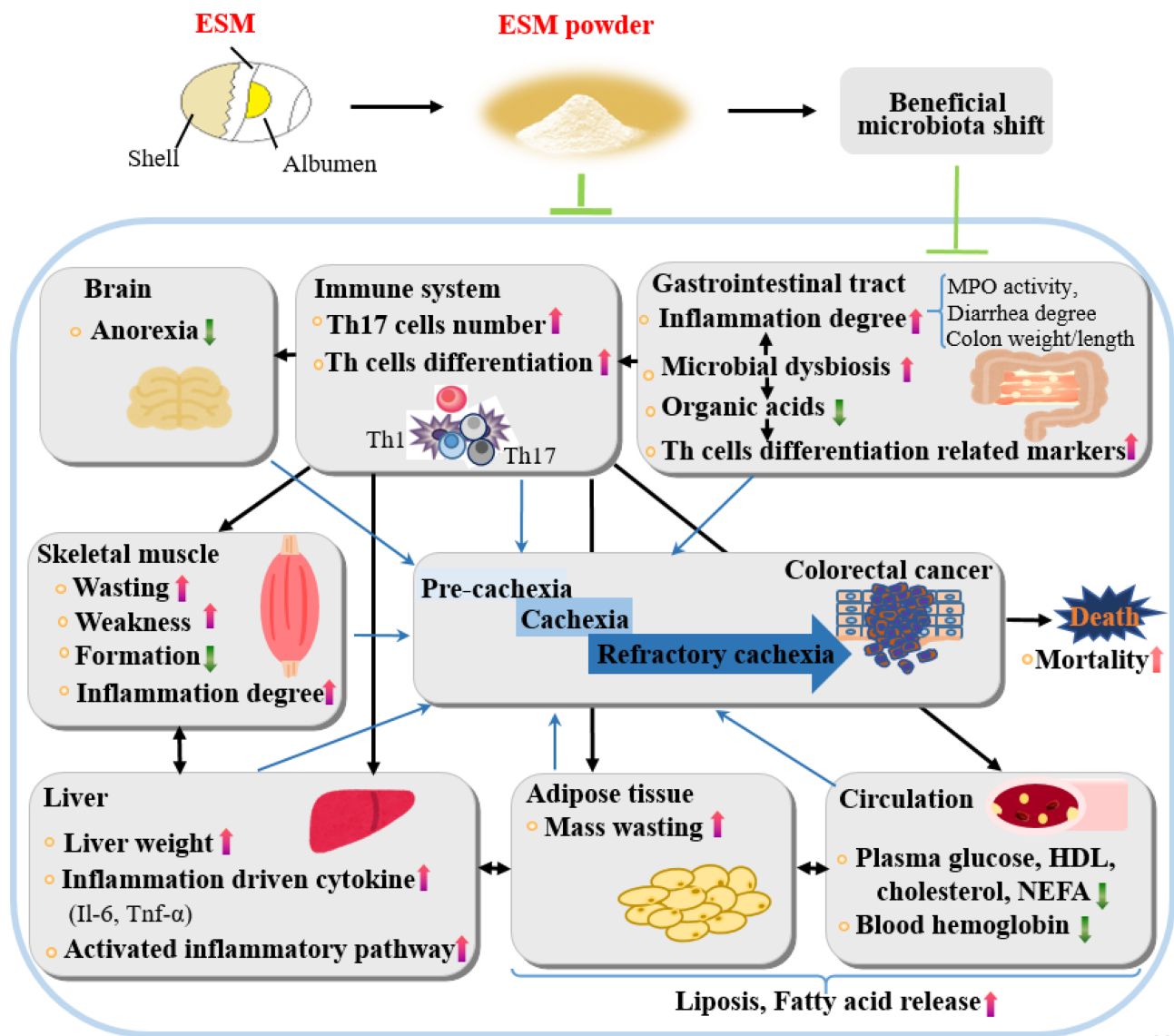


Figure 6 Schematic diagram of the proposed mechanism underlying the suppressing effects of ESM against development of cachexia and cachexia-related symptoms in different organs of IL10-knockout mice.

oneering factors in T cells. BATF enables the binding of IRF4 and IRF8 to AP-1-IRF composite elements in pre-activated CD4⁺ T cells. BATF also directly regulates the expression of several Th-17 cell effector genes.⁴¹ Interestingly, the expression patterns of several genes associated with different components of the complex, including BATF1, IRF4, JUNB and JUND, exhibited the same trends observed in Th-17 generation and IL17 expression, suggesting that BATF pathway downregulation weakened Th-17 differentiation in the KOE group.

Further detailed studies focusing on aspects like anorexia improvement and gut microbiota modulation are required to clarify the action and molecular mechanism of ESM using other animal models. In addition, human studies are neces-

sary to validate the effectiveness and the availability of ESM inferred from animal models. Nevertheless, we presume that our findings could contribute to the prevention of cachexia.

Conclusion

In this study, we used an IL10-knockout mouse model to simulate cachexia and investigated the effect of ESM on cachexia. Our data indicate the association among ESM, attenuation of cachexia-related symptoms in different organs (including the liver, skeletal muscles, gut and immune system)

and a significant shift in the gut microbiota (Figure 6). Given the significant interest in the use of resistant proteins in preventing pre-cachexia, our data offer useful evidence that gut microbiota dysbiosis may serve as an effective target for the prevention and treatment of cachexia.

Acknowledgements

The authors would like to thank Professor Youichiro Wada for his technical assistance at Radioisotope Center, University of Tokyo. The authors of this manuscript certify that they comply with the ethical guidelines for authorship and publishing in *the Journal of Cachexia, Sarcopenia and Muscle*.⁴²

References

- Argiles JM, Lopez-Soriano FJ, Toledo M, Betancourt A, Serpe R, Busquets S. The cachexia score (CASCO): A new tool for staging cachectic cancer patients. *J Cachexia Sarcopenia Muscle* 2011;**2**:87–93.
- Porporato PE. Understanding cachexia as a cancer metabolism syndrome. *Oncogenesis* 2016;**5**:e200.
- Dev R. Measuring cachexia-diagnostic criteria. *Ann Palliat Med* 2019;**8**:24–32.
- Argiles JM, Lopez-Soriano FJ, Busquets S. Counteracting inflammation: A promising therapy in cachexia. *Crit Rev Oncog* 2012; **17**:253–262.
- Blauwhoff-Buskermolen S, de van der Schueren MA, Verheul HM, Langius JA. ‘Pre-cachexia’: A non-existing phenomenon in cancer? *Ann Oncol* 2014;**25**:1668–1669.
- Wang P, Wu P, Siegel MI, Egan RW, Billah MM. IL-10 inhibits transcription of cytokine genes in human peripheral blood mononuclear cells. *J Immunol* 1994;**153**:811–816.
- de Waal Malefyt R, Haanen J, Spits H, Roncarolo MG, te Velde A, Figdor C, et al. Interleukin 10 (IL-10) and viral IL-10 strongly reduce antigen-specific human T cell proliferation by diminishing the antigen-presenting capacity of monocytes via downregulation of class II major histocompatibility complex expression. *J Exp Med* 1991;**174**:915–924.
- Gérard C, Bruyns C, Marchant A, Abramowicz D, Vandenaabeele P, Delvaux A, et al. Interleukin 10 reduces the release of tumor necrosis factor and prevents lethality in experimental endotoxemia. *J Exp Med* 1993;**177**:547–550.
- Fujiki F, Mukaida N, Hirose K, Ishida H, Harada A, Ohno S, et al. Prevention of adenocarcinoma colon 26-induced cachexia by interleukin 10 gene transfer. *Cancer Res* 1997;**57**:94–99.
- Deans DA, Tan BH, Ross JA, Rose-Zerilli M, Wigmore SJ, Howell WM, et al. Cancer cachexia is associated with the IL10-1082 gene promoter polymorphism in patients with gastroesophageal malignancy. *Am J Clin Nutr* 2009;**89**:1164–1172.
- Sun FB, Zhang DL, Zheng HM, Song B. Association of interleukin-10 gene polymorphism with cachexia in patients with gastric cancer. *Zhonghua Zhong Liu Za Zhi* 2010;**32**:845–849.
- Jia H, Takahashi S, Saito K, Kato H. DNA microarray analysis identified molecular pathways mediating the effects of supplementation of branched-chain amino acids on CCl4-induced cirrhosis in rats. *Mol Nutr Food Res* 2013;**57**:291–306.
- Ruff KJ, DeVore DP, Leu MD, Robinson MA. Eggshell membrane: A possible new natural therapeutic for joint and connective tissue disorders. Results from two open-label human clinical studies. *Clin Interv Aging* 2009;**4**:235–240.
- Jia H, Hanate M, Aw W, Itoh H, Saito K, Kobayashi S, et al. Eggshell membrane powder ameliorates intestinal inflammation by facilitating the restitution of epithelial injury and alleviating microbial dysbiosis. *Sci Rep* 2017;**7**:43993.
- Jia H, Aw W, Saito K, Hanate M, Hasebe Y, Kato H. Eggshell membrane ameliorates hepatic fibrogenesis in human C3A cells and rats through changes in PPARgamma-endothelin 1 signaling. *Sci Rep* 2014;**4**:7473.
- Ramli NS, Jia H, Sekine A, Lyu W, Furukawa K, Saito K, et al. Eggshell membrane powder lowers plasma triglyceride and liver total cholesterol by modulating gut microbiota and accelerating lipid metabolism in high-fat diet-fed mice. *Food Sci Nutr* 2020; **8**:2512–2523.
- Melstrom LG, Melstrom KA Jr, Ding XZ, Adrian TE. Mechanisms of skeletal muscle degradation and its therapy in cancer cachexia. *Histol Histopathol* 2007;**22**: 805–814.
- Jakubowski AA, Casper ES, Gabrilove JL, Templeton MA, Sherwin SA, Oettgen HF. Phase I trial of intramuscularly administered tumor necrosis factor in patients with advanced cancer. *J Clin Oncol* 1989;**7**: 298–303.
- Acharyya S, Ladner KJ, Nelsen LL, Damrauer J, Reiser PJ, Swoap S, et al. Cancer cachexia is regulated by selective targeting of skeletal muscle gene products. *J Clin Invest* 2004;**114**:370–378.
- Flores EA, Bistrrian BR, Pomposelli JJ, Dinarello CA, Blackburn GL, Istfan NW. Infusion of tumor necrosis factor/cachectin promotes muscle catabolism in the rat. A synergistic effect with interleukin 1. *J Clin Invest* 1989;**83**:1614–1622.
- Yuen M, Cooper ST, Marston SB, Nowak KJ, McNamara E, Mokbel N, et al. Muscle weakness in TPM3-myopathy is due to reduced Ca²⁺-sensitivity and impaired actoS-myosin cross-bridge cycling in slow fibres. *Hum Mol Genet* 2015;**24**: 6278–6292.
- Ottenheim CA, Lawlor MW, Stienen GJ, Granzier H, Beggs AH. Changes in cross-bridge cycling underlie muscle weakness in patients with tropomyosin 3-based myopathy. *Hum Mol Genet* 2011;**20**: 2015–2025.
- Marco-Ferreres R, Arredondo JJ, Fraile B, Cervera M. Overexpression of troponin T in *Drosophila* muscles causes a decrease in the levels of thin-filament proteins. *Biochem J* 2005;**386**:145–152.
- Qadota H, Benian GM. Molecular structure of sarcomere-to-membrane attachment at

Funding

This work was funded in part by a Grant-in-Aid (18K11095) from the Japan Society for the Promotion of Science (JSPS).

Online supplementary material

Additional supporting information may be found online in the Supporting Information section at the end of the article.

Conflict of interest

The authors declare no conflict of interest.

- M-Lines in *C. elegans* muscle. *J Biomed Biotechnol* 2010;**2010**:864749.
25. Tomasi M, Canato M, Paolini C, Dainese M, Reggiani C, Volpe P, et al. Calsequestrin (CASQ1) rescues function and structure of calcium release units in skeletal muscles of CASQ1-null mice. *Am J Physiol Cell Physiol* 2012;**302**:C575–C586.
 26. Ravenscroft G, Zaharieva IT, Bortolotti CA, Lambrughi M, Pignataro M, Borsari M, et al. Bi-allelic mutations in MYL1 cause a severe congenital myopathy. *Hum Mol Genet* 2018;**27**:4263–4272.
 27. Frey N, Frank D, Lippl S, Kuhn C, Kögler H, Barrientos T, et al. Calcineurin-2 deficiency increases exercise capacity in mice through calcineurin/NFAT activation. *J Clin Invest* 2008;**118**:3598–3608.
 28. Ding J, Cong YF, Liu B, Miao J, Wang L. Aberrant protein turn-over associated with myofibrillar disorganization in FHL1 knock-out mice. *Front Genet* 2018;**9**:273.
 29. Gong YY, Liu YY, Li J, Su L, Yu S, Zhu XN, et al. Hypermethylation of Cox5a promoter is associated with mitochondrial dysfunction in skeletal muscle of high fat diet-induced insulin resistant rats. *PLoS ONE* 2014;**9**:e113784.
 30. Shearer J, Fueger PT, Bracy DP, Wasserman DH, Rottman JN. Partial gene deletion of heart-type fatty acid-binding protein limits the severity of dietary-induced insulin resistance. *Diabetes* 2005;**54**:3133–3139.
 31. Gu P, Theiss A, Han J, Feagins LA. Increased cell adhesion molecules, PECAM-1, ICAM-3, or VCAM-1, predict increased risk for flare in patients with quiescent inflammatory bowel disease. *J Clin Gastroenterol* 2017;**51**:522–527.
 32. Tisdale MJ. Cachexia in cancer patients. *Nat Rev Cancer* 2002;**2**:862–871.
 33. Patra SK, Arora S. Integrative role of neuropeptides and cytokines in cancer anorexia-cachexia syndrome. *Clin Chim Acta* 2012;**413**:1025–1034.
 34. Mukwaya A, Lennikov A, Xeroudaki M, Mirabelli P, Lachota M, Jensen L, et al. Time-dependent LXR/RXR pathway modulation characterizes capillary remodeling in inflammatory corneal neovascularization. *Angiogenesis* 2018;**21**:395–413.
 35. Klein GL, Petschow BW, Shaw AL, Weaver E. Gut barrier dysfunction and microbial translocation in cancer cachexia: a new therapeutic target. *Curr Opin Support Palliat Care* 2013;**7**:361–367.
 36. Kitamura T, Fujishita T, Loetscher P, Revesz L, Hashida H, Kizaka-Kondoh S, et al. Inactivation of chemokine (C-C motif) receptor 1 (CCR1) suppresses colon cancer liver metastasis by blocking accumulation of immature myeloid cells in a mouse model. *Proc Natl Acad Sci USA* 2010;**107**:13063–13068.
 37. Bindels LB, Delzenne NM. Muscle wasting: The gut microbiota as a new therapeutic target? *Int J Biochem Cell Biol* 2013;**45**:2186–2190.
 38. Zhang M, Zhou Q, Dorfman RG, Huang X, Fan T, Zhang H, et al. Butyrate inhibits interleukin-17 and generates Tregs to ameliorate colorectal colitis in rats. *BMC Gastroenterol* 2016;**16**:84.
 39. Zheng Y, Rudensky AY. Foxp3 in control of the regulatory T cell lineage. *Nat Immunol* 2007;**8**:457–462.
 40. Bettelli E, Carrier Y, Gao W, Korn T, Strom TB, Oukka M, et al. Reciprocal developmental pathways for the generation of pathogenic effector TH17 and regulatory T cells. *Nature* 2006;**441**:235–238.
 41. Li P, Spolski R, Liao W, Wang L, Murphy TL, Murphy KM, et al. BATF-JUN is critical for IRF4-mediated transcription in T cells. *Nature* 2012;**490**:543–546.
 42. von Haehling S, Morley JE, Coats AJS, Anker SD. Ethical guidelines for publishing in the Journal of Cachexia, Sarcopenia and Muscle: update 2021. *J Cachexia Sarcopenia Muscle* 2021;**12**:2259–2261.